Available online at www.sciencedirect.com
ScienceDirect
International Journal of Heat and Mass Transfer 50 (2007) 1649–1655
International Journal of HEAT and MASS TRANSFER
www.elsevier.com/locate/ijhmt

Natural convection with distributed heat source modulation

A. Bazylak, N. Djilali *, D. Sinton

Institute for Integrated Energy Systems and Department of Mechanical Engineering, University of Victoria, P.O. Box 3055 STN CSC, Victoria, BC, Canada V8W 3P6

Received 3 February 2006; received in revised form 21 October 2006
Available online 29 December 2006

Abstract

The heat transfer associated with an infinite planar array of distributed heat sources on the bottom wall of a horizontal air filled plenum is modelled numerically, and simulations which account for natural convection and radiation are performed to investigate the effect of independent sinusoidal modulation of heat fluxes. Nusselt number, maximum velocity and Rayleigh number decrease with increasing oscillation amplitude, while the temperature difference between the cold upper wall and the average source temperature decreases. The decrease in temperature difference associated with heat flux modulation indicates an improvement in overall heat transfer.

Keywords: Natural convection; Heat transfer; Heat modulation; Electronic packaging

1. Introduction

Unsteady heat generation is common in electronic components [1], and more importantly, small-scale systems can be designed to induce dynamic heat fluxes. The design of more efficient passive cooling for high density packaging of electronic devices can be improved by taking advantage of these dynamic heat fluxes to generate thermal instabilities, which will result in improved rates of heat transfer. The potential of oscillating or vibrating walls to enhance heat transfer in enclosures has been the subject of a number of studies, e.g. [2,3]. The focus of this study is the enhancement of natural convection based heat transfer through independent modulation of heat fluxes from a planar array of distributed heat sources.

Many studies have been performed on horizontal fluid layers heated from below with oscillating temperature boundary conditions. Rosentblat and Tanaka [4] investigated thermal convection associated with an incompressible fluid confined between two parallel, horizontal and rigid planes that extend infinitely in the horizontal direction. They found that bottom wall temperature modulations of high amplitude and low frequency delayed the onset of instability in the flow field. Mantle et al. [5] investigated the effects of temperature modulation on natural convection in a horizontal water layer heated from below. Experiments were performed in which the bottom wall temperature varied in a "sawtoothlike" fashion, and they found that the period of oscillation has no effect on heat transfer rates when the amplitude of fluctuation is small, but the period has a large effect when the amplitude of fluctuation is large. Transient convective heat transfer in a cavity subjected to sinusoidal temperature modulations was investigated numerically by Lakhal et al. [6] and more recently by Soong et al. [7]. Larger amplitude and lower frequency modulations were found to induce a stabilizing effect, in agreement with previous work by Rosentblat and Tanaka [4]. Bae and Hyun [8] presented a time-dependent two-dimensional numerical study on laminar natural convection air-cooling in a vertical rectangular enclosure with discrete flush-mounted heaters on one side of the wall. Three heaters were situated on the sidewall, and the lowest elevated source was switched 'on' and 'off', while the others were kept 'on'. According to Bae and Hyun [8], a discretely heated vertical wall leads to a higher heat transfer

* Corresponding author. Tel.: +1 250 721 6034; fax: +1 250 721 6323.
E-mail address: ndjilali@uvic.ca (N. Djilali).

0017-9310/$ - see front matter © 2006 Elsevier Ltd. All rights reserved.
doi:10.1016/j.ijheatmasstransfer.2006.10.033

Nomenclature

B	mean amplitude of heat flux modulation
C_p	specific heat capacity
$\vec{g}$	acceleration of gravity
h	heat transfer coefficient $\left(= q_i''(t)/T_S(x,t) - T_C\right)$, $i = 1,2$
I	radiation intensity
I_0	boundary condition intensity
I_{in}	incident radiation intensity
k	thermal conductivity
L	length of heat source, plenum height and spacing length
n	index of refraction
$\vec{n}$	normal vector
Nu	spatially-averaged Nusselt number
Nu_{avg}	temporally-averaged and spatially-averaged Nusselt number
P	static pressure
Pr	Prandtl number
$q_i''(t)$	source heat flux, $i = 1,2$
q_{in}''	incident radiative heat flux at wall
q_{out}''	radiative flux leaving wall
q_S''	spacing heat flux
Ra	Rayleigh number
$\vec{s}$	direction vector
$\vec{s}'$	scattering direction vector
$\vec{r}$	position vector
T	temperature
T_C	top wall temperature
T_{max}	maximum temperature of heat source surface
T_w	wall temperature
t	time
V_{max}	maximum velocity
$V_{max,avg}$	temporally averaged maximum velocity
$\vec{v}$	velocity

Greek symbols

α	hemispherical surface absorptivity
α^*	thermal diffusivity of air
β	thermal expansion coefficient
ΔT	difference between local temperature and top wall temperature $(= T - T_L)$
$\Delta T_{max,avg}$	temporally-averaged maximum temperature difference between heat source and top wall temperature
δ	oscillation amplitude
ε	hemispherical surface emissivity
Φ	phase function
θ	phase shift
Ω'	solid angle
ρ	fluid density
σ	Stefan–Boltzmann constant $(5.672 \times 10^{-8}$ W/m^2 K$^4)$
σ_s	scattering coefficient
τ	period of oscillation
υ	kinematic viscosity of air
ω	frequency of modulation

coefficient than a fully heated vertical wall, which was also shown by Keyhani et al. [9]. Shu et al. [10] presented experimental and numerical investigations on natural convection in a rectangular cavity with oscillating left-wall temperatures. Numerical simulations were used to study the effects on modulation frequency and Prandtl number on the fluid flow. The authors considered a water-filled rectangular cavity with adiabatic top and bottom surfaces. The right side was kept at a constant temperature, and the left side had a sinusoidally oscillating temperature boundary condition. They found that the flow oscillation in the cavity strongly depends on the frequency of temperature perturbation applied to the boundary, where the flow modulation is weaker at high frequencies of temperature oscillation. Roppo et al. [11] presented an analytical study of Rayleigh–Bénard convection in a thin liquid layer heated from below, where the lower boundary is modulated sinusoidally in time. The horizontal layer of fluid extended infinitely in the horizontal direction between two parallel planes. The top wall was kept at a constant lower temperature, and the lower plate oscillated sinusoidally about a nonzero mean value. With the trend towards electronic miniaturization and increasing component density, the number of components asymptotically approaches an infinite value. In this paper, the constraint of sidewalls is removed, effectively considering an infinite array of distributed heat sources and their effects on heat transfer.

In this work, computational fluid dynamics (CFD) is applied to investigate the effects on heat transfer when the heat flux boundary conditions for an infinite array of distributed heat sources in a horizontal air filled plenum are modulated with respect to time. This work indicates the potential to improve passive heat removal through natural convection by triggering thermal instabilities through heat flux modulation.

2. Modelling approach

Fig. 1 illustrates the geometric and thermal boundary conditions of the two-dimensional problem under consideration. Flush-mounted heat sources of equal length, L, have prescribed uniform heat flux boundary conditions, $q_1''(t)$ and $q_2''(t)$. The heat source length, spacing length and plenum height have a 1:1:1 ratio. This configuration is characteristic of electronics applications, as discussed in a recent investigation where source spacings and source sizes were studied as the parameters governing steady state Rayleigh–Bénard natural convection [12]. For all simulations

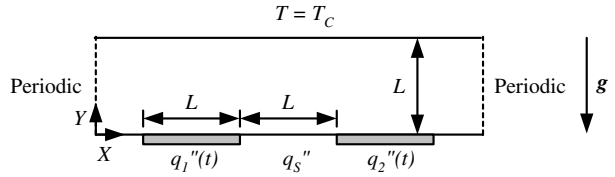

Fig. 1. Schematic of the two-dimensional computational domain showing geometric and thermal boundary conditions.

including the effects of thermal radiation, air is assumed to be non-participating (absorption and scattering coefficients are zero), and the index of refraction ($n = 1$) is assumed to be constant over all wavelengths and temperatures. All surfaces are opaque and gray-diffuse, with hemispherical emissivity, ε, and absorptivity, α, values the same for all surfaces.

The following conditions are prescribed on the other boundaries:

- bottom wall, between sources: zero heat flux boundary condition, $q''_S = 0$;
- top wall: constant temperature, T_C;
- bottom and top walls: no-slip velocity condition;
- side boundaries: periodic boundary condition.

The periodicity condition simulates an effectively infinite array of heat sources without the influence of sidewalls. In this work, the maximum temperature difference, ΔT, is assumed small enough to justify the use of the Boussinesq approximation. The resulting continuity, momentum and energy equations governing the flow and heat transfer are given by

$$\nabla \cdot \vec{v} = 0 \tag{1}$$

$$\frac{\partial \vec{v}}{\partial t} + \nabla \cdot (\vec{v}\ \vec{v}) = -\frac{1}{\rho}\nabla P + \nabla \cdot (\upsilon \nabla \vec{v}) + \beta \Delta T\, \vec{g} \tag{2}$$

where $\vec{v}$ is the velocity vector, t is the time, ρ is the fluid density, P is the static pressure, υ is the kinematic viscosity, β is the thermal expansion coefficient, and $\vec{g}$ is the acceleration of gravity.

$$\rho C_p \left(\frac{\partial T}{\partial t} + \vec{v} \cdot \nabla T \right) = k \nabla^2 T \tag{3}$$

where C_p is the specific heat capacity, k is the thermal conductivity and T is the temperature.

The Discrete Ordinates model is used to solve the radiative heat transfer equation

$$\nabla \cdot (I(\vec{r},\vec{s})\vec{s}) + (\alpha + \sigma_s) I(\vec{r},\vec{s}) = \alpha n^2 \frac{\sigma T^4}{\pi} + \frac{\sigma_s}{4\pi} \int_0^{4\pi} I(\vec{r},\vec{s}')\Phi(\vec{s}\cdot\vec{s}')\,\mathrm{d}\Omega' \tag{4}$$

where I, $\vec{r}$, $\vec{s}$, $\vec{s}'$, α, σ_s, σ, Φ, and Ω' are the radiation intensity, position vector, direction vector, scattering direction vector, adsorption coefficient, scattering coefficient, Stefan–Boltzmann constant (5.672×10^{-8} W/m^2 K^4), phase function and solid angle, respectively.

The incident radiative heat flux at the wall is given by

$$q''_{\text{in}} = \int_{\vec{s}\cdot\vec{n}>0} I_{\text{in}} \vec{s} \cdot \vec{n}\,\mathrm{d}\Omega \tag{5}$$

where I_{in} is the incident radiation intensity. The net radiative heat flux leaving the wall is given by

$$q''_{\text{out}} = (1-\varepsilon) q''_{\text{in}} + n^2 \varepsilon_w \sigma T_w^4 \tag{6}$$

where ε is the wall emissivity coefficient, and T_w is the temperature at the wall. The boundary condition intensity is calculated by

$$I_0 = \frac{q''_{\text{out}}}{\pi} \tag{7}$$

The heat transfer from the sources is expressed in terms of the Nusselt number averaged over the area of the source, which is defined as

$$Nu = \frac{hL}{k} \tag{8}$$

where L is the characteristic length of the system (as labeled in Fig. 1), and h, the heat transfer coefficient is defined as

$$h(x,t) = \frac{q''_i(t)}{T(x,t) - T_C} \tag{9}$$

where $i = 1, 2$. The temporally-averaged and spatially-averaged Nusselt number is given by

$$Nu_{\text{avg}} = \frac{1}{\tau}\int_0^\tau \frac{1}{L}\int_0^L Nu(x,t)\,\mathrm{d}x\,\mathrm{d}t \tag{10}$$

where τ is the period of oscillation. The Rayleigh number is defined as

$$Ra = \frac{g\beta(T_{\max} - T_C)L^3}{\alpha^* \nu} \tag{11}$$

where $T_{\max}$ is the maximum temperature on the surface of the heat source, and α^* is the thermal diffusivity of air. The Rayleigh number is calculated *a posteriori* once $T_{\max}$ has been determined from the simulations. Although the results have been non-dimensionalized to apply to any length scale, in the context of the air properties and temperature differences of interest, the length scale ranges from 500 μm to 10 mm. The Prandtl number has a value of 0.74 and is given by

$$Pr = \frac{\nu}{\alpha} \tag{12}$$

This model was implemented in FLUENT, a commercial finite-volume based CFD package [13]. The governing equations were solved using the QUICK scheme. For steady state simulations PRESTO was used, and for time-dependent simulations the PISO algorithm was used to solve for the pressure. A hexagonal grid and segregated solver were used for all simulations. For time-dependent simulations, a second order implicit formulation was used with constant time steps of 10^{-2} s. In a previous study

focusing on steady state convection over distributed heat sources [12], a systematic grid dependence study showed that variations of the 0.1% were obtained when using a 25×100 mesh compared to a 60×240 mesh. In the current unsteady simulations, the characteristic size of the flow patterns is similar, and a mesh of 30×120 was used for all simulations.

3. Heat flux modulation

At very low modulation frequencies, the system approaches the steady state case, which is characterized in Fig. 2. The curves marked by triangles are the heat transfer results without thermal radiation and mark the onset of thermal instability with a critical Rayleigh number of 810. The curves marked by circles are the results with thermal radiation assuming gray-diffuse surfaces with $\varepsilon = 0.5$. The divergence of the curves marked by circles shows the effect of natural convection and the onset of thermal instability, which occurs at a critical Rayleigh number of 880. Finally, the curves marked by squares show the effect on heat transfer when assuming gray-diffuse surfaces with $\varepsilon = 1$. Here, the onset of thermal instability occurs at a critical Rayleigh number of 1220. It is important to note that increasing

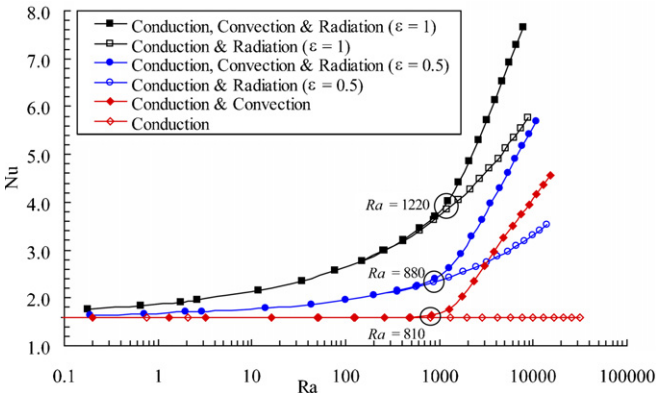

Fig. 2. Average Nusselt number versus Rayleigh number, showing the effects of thermal radiation on thermal instability and heat transfer rates.

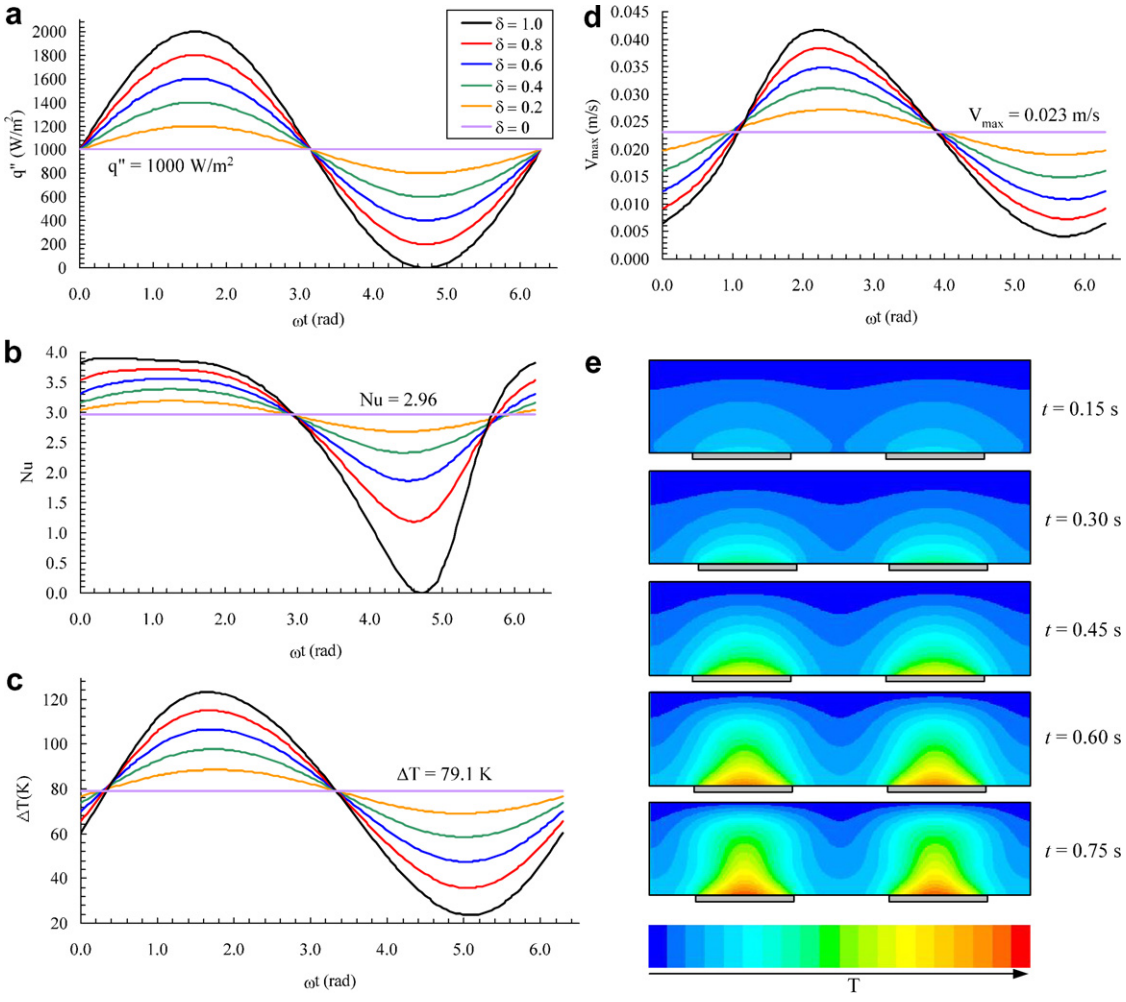

Fig. 3. Heat transfer effects from varying the heat flux oscillation amplitude about the steady state value, $\delta = 0$. Results are shown for varying oscillation amplitudes over one full period: (a) heat flux boundary condition, (b) spatial average of Nusselt number, (c) temperature difference between cold upper wall and area weighted average source temperature, (d) maximum velocity, and (e) time sequenced temperature contours for $\delta = 1$.

thermal radiation delays the onset of thermal instability in the system, which is consistent with work presented in [14,15]. When radiation is included in the numerical model, the transition becomes smoother, and as expected, the heat transfer rates are significantly higher. Thermal radiation is included in all subsequent simulations.

The effects of source heat flux modulation are studied for an operating point well within the convection-dominated regime. The source heat flux boundary conditions are modulated with respect to time for the configuration shown in Fig. 1, where $\varepsilon = 0.5$, $L = 6$ mm, $\Delta T = 90$ K, and $Ra = 1560$. The heat flux boundary conditions stipulate a uniform heat flux profile along each heat source. In the following investigation, all heat sources are modulated by the same frequency, ω. A 1.5 s period of oscillation was employed because it is characteristic of the time required for this system to approach steady state. In the context of the numerical simulations this period represents 150 time steps.

The heat flux boundary conditions for each heat source are modulated sinusoidally with alternating heat sources phase shifted by an angle, θ. The heat fluxes of alternating sources are given by

$$q_1''(t) = B[1 + \delta \sin(\omega t)] \tag{13}$$

$$q_2''(t) = B[1 + \delta \sin(\omega t + \theta)] \tag{14}$$

where B is the mean amplitude of heat flux modulation.

Fig. 3 shows the effects on heat transfer when the oscillation amplitude of heat flux modulation varies between values $0 \leqslant \delta \leqslant 1$, when both $q_1''(t)$ and $q_2''(t)$ are in phase, i.e. $\theta = 0$. Fig. 3a shows the imposed heat flux boundary conditions of each heat source over one period. Fig. 3b shows Nu for one period, which varies non-linearly with the applied heat flux modulation at higher amplitudes. Also over one period, Fig. 3c shows the resulting temperature difference between the cold upper wall and the area weighted average source temperature, and Fig. 3d shows

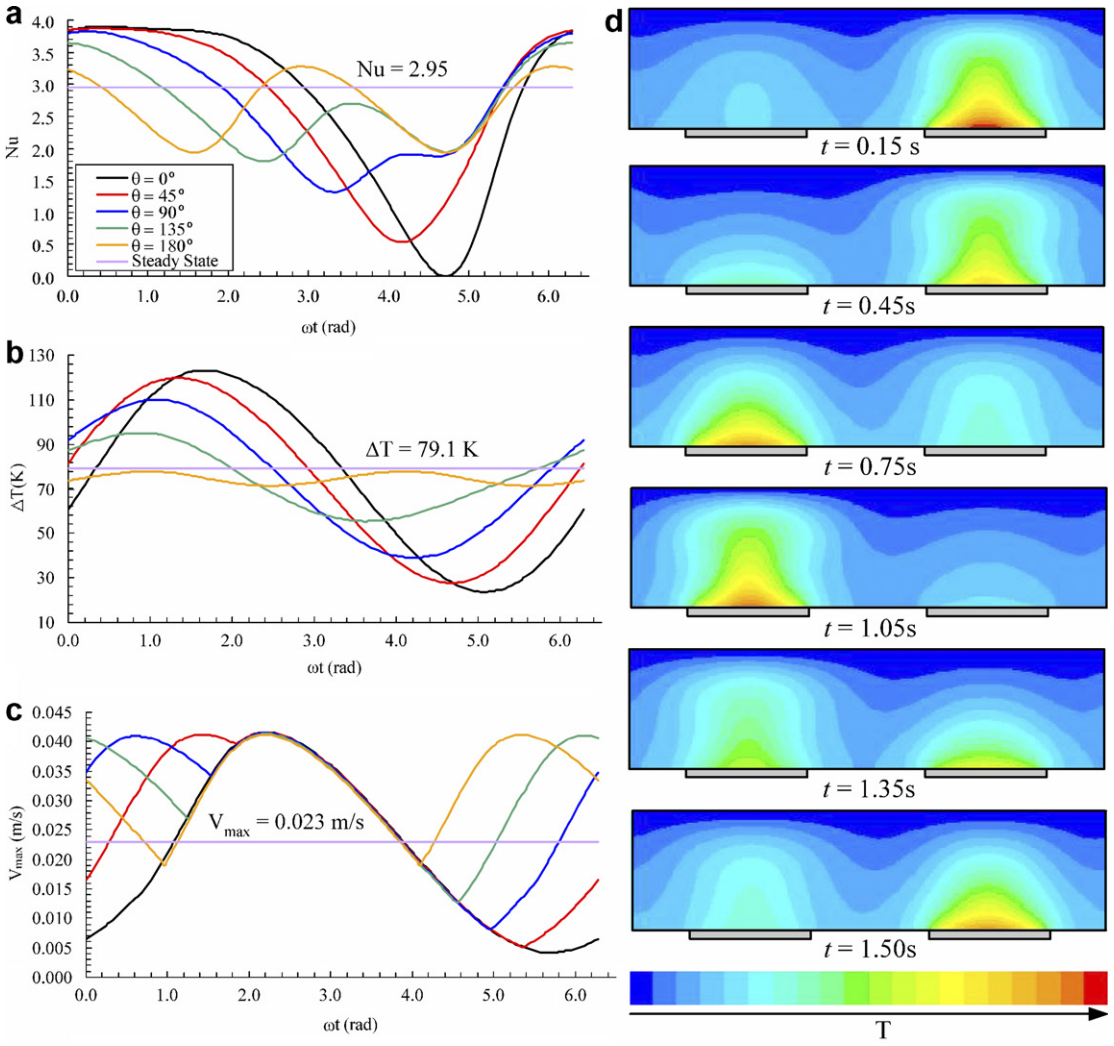

Fig. 4. Source heat flux sinusoidal modulation effects on heat and mass transfer for alternating sources shifted by 0°, 45°, 90°, 135° and 180° for one period: (a) spatial average of Nusselt number, (b) temperature difference between cold upper wall and area weighted average source temperature, (c) maximum velocity magnitude, and (d) time sequenced temperature contours for $\theta = 180°$.

the maximum velocity that occurs in the system. Fig. 3e illustrates time sequenced temperature contours, which show the evolution of thermal plumes for the case where $\delta = 1$ and $\theta = 0°$. The temperature difference between the cold upper wall and the area weighted average source temperature decreases as the oscillation amplitude increases. Averaged over one period of time, $\Delta T_{max,avg}$ decreases by 2%, 4%, and 5%, for oscillation amplitudes of $\delta = 0.6$, 0.8, and 1.0, respectively. This decrease in temperature difference shows an improvement in heat transfer from the heat sources. However, for $\delta \leqslant 0.6$, $\Delta T_{max,avg}$ decreases by less than one percent compared to the steady state case. Compared to the steady state case where $\delta = 0$, average values over one period of time of Nu_{avg}, V_{max} and Ra decrease with increasing oscillation amplitude. For $\delta = 1$, Nu_{avg}, V_{max} and Ra decrease by 9%, 7%, and 6%, respectively. The oscillation amplitude value of $\delta = 1$ was used for all subsequent simulations because it resulted in the largest decrease in average temperature.

Fig. 4 shows the effect of varying the heat flux boundary condition phase shift of adjacent heat sources on Nu, $\Delta T_{max,avg}$ and V_{max} over a range of Rayleigh numbers. Over one period of time, Fig. 4a shows the spatially averaged Nu, Fig. 4b shows the temperature difference between the cold upper wall and the area weighted source temperature, and Fig. 4c shows the maximum velocity magnitude in the system. Fig. 4d illustrates time sequenced temperature contours, which show the evolution of thermal plumes for the case where $\delta = 1$ and $\theta = 180°$. Compared to the steady state case, Nu_{avg} decreases by approximately 10% when a phase shift is introduced. Even though Nu_{avg} decreases, the temperature difference between the cold upper wall and the average source temperature is 6% less compared to that at steady state. This significant decrease in $\Delta T_{max,avg}$ indicates that using a large oscillation amplitude and introducing a phase shift between the heat flux boundary conditions of adjacent heat sources is a promising method of enhancing passive heat removal from heat generating components. Over one period of time, the average maximum velocity, $V_{max,avg}$, increases by 28%, 38%, and 41% when the heat flux boundary conditions of adjacent heat sources are phase shifted by 90°, 135° and 180°, respectively. This significant increase in $V_{max,avg}$ is also promising as a method for enhancing the mass transfer above the heat sources.

4. Conclusions

This work brings new insight on the heat transfer effects of modulating the heat flux boundary conditions of an infinite array of distributed flush-mounted heat sources on the bottom wall of a horizontal air filled plenum. It was found that Nusselt number, maximum velocity and Rayleigh number decrease with increasing oscillation amplitude, while the temperature difference between the cold upper wall and the average source temperature decreases. This decrease in temperature difference indicates an improvement in overall heat transfer from the heat sources.

Since the Nusselt number in this work is averaged temporally and spatially, it is no longer an ideal measure of heat transfer in the system. Due to the time and space averaging, one cannot assume that an increase in Nu_{avg} results from an inversely proportional decrease in the temperature difference in the system. For the time-dependent situations studied in this work, the best measure of heat transfer improvements is the maximum temperature difference in the system. When designing electronic components with high-heat fluxes, the maximum temperature that the device can withstand is often a major operating limitation. The time-averaged maximum temperature value is also of interest simply because the temperature of the heat source oscillates about a median value. Both values have been included in this analysis because they are useful for measuring the improvement in heat transfer.

When a phase shift is introduced between alternating heat sources, the Nusselt number decreases by approximately 10%. The temperature difference between the cold upper wall and the average source temperature is less than that at steady state by 6%. The maximum velocity increases by 41% when the heat sources are out of phase by 180°. It is important to note that a decrease in temperature difference is observed, and an increase in maximum velocity is observed, both of which are desirable for heat removal and mass transport in small-scale electronics.

Acknowledgements

The authors are grateful for the financial support of the Natural Sciences and Engineering Research Council (NSERC) of Canada, through a post-graduate scholarship to A. Bazylak and research grants to N. Djilali and D. Sinton. Financial support from the University of Victoria, through post-graduate scholarships to A. Bazylak, is also gratefully acknowledged.

References

[1] M.J. Vesligaj, C.H. Amon, Transient thermal management of temperature fluctuations during time varying workloads on portable electronics, IEEE Trans. Comp. Pack. Technol. 22 (4) (1999) 541–550.
[2] L.A. Florio, A. Harnoy, Feasibility study of unconventional cooling of electronic components by vibrating plates at close proximity, Numer. Heat Transfer, Part A: Appl. 47 (2005) 997–1024.
[3] C.-H. Cheng, K.-S. Hung, Numerical prediction of thermal convection in a rectangular enclosure with oscillating wall, Numer. Heat Transfer, Part A: Appl. 48 (2005) 791–809.
[4] S. Rosentblat, G.A. Tanaka, Modulation of thermal convection instability, Phys. Fluids 14 (7) (1971) 1319–1322.
[5] J. Mantle, M. Kazmierczak, B. Hiawy, The effect of temperature modulation on natural convection in a horizontal layer heated from below: high-Rayleigh-number experiments, J. Heat Transfer 116 (1994) 614–620.
[6] E.K. Lakhal, M. Hasnaoui, P. Vasseur, E. Bilgen, Natural convection in a square enclosure heated periodically form part of the bottom wall, Numer. Heat Transfer, Part A: Appl. 27 (1995) 319–333.

[7] C.Y. Soong, P.Y. Tzeng, C.D. Hsieh, Numerical study of bottom-wall temperature modulation effects on thermal instability and oscillatory cellular convection in a rectangular enclosure, Int. J. Heat Mass Transfer 44 (2001) 3855–3868.
[8] J.H. Bae, J.M. Hyun, Time dependent buoyant convection in an enclosure with discrete heat sources, Int. J. Therm. Sci. 43 (2004) 3–11.
[9] M. Keyhani, V. Prasad, R. Cox, An experimental study of natural convection in a vertical cavity with discrete heat sources, J. Heat Transfer 100 (1988) 616–624.
[10] Y. Shu, B.Q. Li, B.R. Ramaprian, Convection in modulated thermal gradients and gravity: experimental measurements and numerical simulations, Int. J. Heat Mass Transfer 48 (2005) 145–160.
[11] M.N. Roppo, S.H. Davis, S. Rosenblat, Bénard convection with time-periodic heating, Phys. Fluids 27 (4) (1984) 796–803.
[12] A. Bazylak, N. Djilali, D. Sinton, Natural convection in an enclosure with distributed heat sources, Numer. Heat Transfer, Part A: Appl. 49 (2006) 655–667.
[13] FLUENT Inc., Lebanon, NH. Fluent 6.1.22, 2003.
[14] V. Borget, F. Bdéoui, A. Soufiani, The transverse instability in a differentially heated vertical cavity filled with molecular radiating gases. I. Linear stability analysis, Phys. Fluids 13 (5) (2001) 1492–1507.
[15] C.H. Lan, O.A. Ezekoye, J.R. Howell, K.S. Ball, Stability analysis for three-dimensional Rayleigh–Bénard convection with radiatively participating medium using spectral methods, Int. J. Heat Mass Transfer 46 (2003) 1371–1383.